

Formation Mechanism of Guided Resonances and Bound States in the Continuum in Photonic Crystal Slabs

Xingwei Gao^{1†}, Chia Wei Hsu^{2,3*}, Bo Zhen^{2,4}, Xiao Lin^{1,2}, John D. Joannopoulos², Marin Soljačić² and Hongsheng Chen^{1*}

¹The Electromagnetics Academy at Zhejiang University, Zhejiang University, Hangzhou 310027, China

²Research Laboratory of Electronics, Massachusetts Institute of Technology, Cambridge, Massachusetts 02139, USA

³Department of Applied Physics, Yale University, New Haven, Connecticut 06520, USA

⁴Physics Department and Solid State Institute, Technion, Haifa 32000, Israel.

*Correspondence: Chia Wei Hsu, Email: chiawei.hsu@yale.edu; or Hongsheng Chen, Email: hansomchen@zju.edu.cn

We develop a formalism, based on the mode expansion method, to describe the guided resonances and bound states in the continuum (BICs) in photonic crystal slabs with one-dimensional periodicity. This approach provides analytic insights to the formation mechanisms of these states: the guided resonances arise from the transverse Fabry-Pérot condition, and the divergence of the resonance lifetimes at the BICs is explained by a destructive interference of radiation from different propagating components inside the slab. We show BICs at the center and on the edge of the Brillouin zone protected by symmetry, as well as BICs at generic wave vectors not protected by symmetry.

Key words: bounded states in the continuum; photonic crystal; mode expansion; quality factor; guided resonance

Introduction

Conventionally, the confinement of waves is achieved by spectrally separating the bound state away from the continuum of radiating waves that can carry energy away—examples include electronic bound states at negative energies and light guided below the light line or inside a photonic bandgap. Bound states in the continuum (BICs) are special states that remain localized and have infinite lifetimes even though they reside inside the continuum¹. Historically, BIC was first proposed by von Neumann and Wigner for an electron in an engineered potential², although such an electron BIC has never been achieved. More recently, optical BICs have been

experimentally realized in a range of photonic systems³⁻⁹, although the definition of BICs in periodic structures is not identical to the original definition of BIC in an isolated structure¹⁰. In periodic structures, BICs may be found by varying the incident angle without tuning the structure, which makes their realization relatively simple^{3,5,6,11-22}. Photonic crystal (PhC) slabs—dielectric slabs with periodically modulated refractive index^{11,23,24}—are particularly attractive given their macroscopic sizes and ease of fabrication. The guided resonances and BICs in PhC slabs have been used for a wide range of applications from lasers²⁵⁻¹⁹ to sensors^{13,30,31} and filters³². The wave confinement mechanisms of BICs are distinct from those of conventional bound states. In the presence of multiple resonances, BICs can arise from the destructive interference of radiation from the different resonances^{13-16,33,34}. However, when only one resonance is present, the theoretical studies of BICs rely on numerical simulations that are time consuming and provide little insight to the formation mechanism. Here, we develop a mode expansion method that is capable of describing guided resonances and BICs in slabs quantitatively without any other approximations except for a truncation of the basis size, and yet it also provides the fast speed and insights of an analytic model. In this formalism, guided resonances require the round-trip transverse phase shift for each in-slab propagating mode to be an integer multiple of 2π , and BICs can be understood as arising from the destructive interference of radiation from different propagating waves inside the slab. We also apply this approach to predict optical BICs in periodic inhomogeneous backgrounds, where BICs can be found both at the center and on the edge of the Brillouin zone due to symmetry protection, as well as inside the Brillouin zone where they are not protected by symmetry. Although we only show examples for systems with one dimensional periodicity, our mode-expansion method can be easily extended into systems that are periodic in two dimensions.

Materials and Methods

Mode expansion method

For simplicity, we consider TM modes (with electric fields $\mathbf{E} = E_z \hat{z}$) in a PhC slab that is periodic in y and uniform in z (Fig. 1a); the generalization to TE modes and to PhC slabs with two-dimensional periodicity is straightforward. We consider structures that are mirror symmetric in the normal direction x (this symmetry is necessary to reduce the number of radiation channels⁶) and where the slab permittivity $\varepsilon_1(y)$ does not vary in the normal direction (common in most fabricated structures of PhC slabs). Here we

consider two cases: the permittivity of the surrounding medium $\varepsilon_2(y)$ is a constant (Fig. 1b) or is periodic with the same period a as the slab (Fig. 1c). Any field profile satisfying the wave equation $[\nabla^2 + \varepsilon(x, y)k_0^2]E_z = 0$ can always be expanded in the basis of the eigenmodes of $\varepsilon_1(y)$ and $\varepsilon_2(y)$ -where $k_0 = \omega/c$, is the frequency, and c is the vacuum speed of light. For an even-in- x TM mode with wave vector k_y , we can write

$$E_z(x, y) = e^{ik_y y} \begin{cases} \sum_m C_m \frac{\cos(\beta_m x)}{\cos(0.5\beta_m h)} u_m(y), & 0 \leq x < 0.5h, \\ \sum_m T_m e^{i\gamma_m(x-0.5h)} \vartheta_m(y), & x > 0.5h, \end{cases} \quad (1)$$

where h is the slab thickness. Here, $u_m(y)$, $\vartheta_m(y)$, β_m and γ_m are eigenfunctions and propagation constants inside and outside the slab:

$$\hat{H}_1 u_m(y) = \beta_m^2 u_m(y), \quad (2.1)$$

$$\hat{H}_2 \vartheta_m(y) = \gamma_m^2 \vartheta_m(y), \quad (2.2)$$

with $\hat{H}_l = (\partial/\partial y + ik_y)^2 + k_0^2 \varepsilon_l(y)$ for $l = 1, 2$. \hat{H}_1 and \hat{H}_2 are Hermitian operators subject to periodic boundary condition $u_m(y + a) = u_m(y)$, $\vartheta_m(y + a) = \vartheta_m(y)$. For a given frequency and k_y , there will be a finite number of eigenmodes with $\beta_m^2 > 0$ (or $\gamma_m^2 > 0$) that propagate in the x direction, with an infinite number of eigenmodes with $\beta_m^2 < 0$ (or $\gamma_m^2 < 0$) that are evanescent in x . Similar expansion methods were used previously in Reference.35 for water waves and for quantum waveguides. In Eq. (1), we impose the outgoing boundary condition (no incoming wave outside the slab) to restrict our analysis to leaky guided resonances and bound states. Odd-in- x TM modes can be written similarly by replacing the cosine in Eq. (1) with sine. C_m and T_m are coefficients of the eigenmode expansion, and they can be determined via the continuity of E_z and $\partial E_z/\partial x$ at $x = 0.5h$, which requires

$$\sum_m C_m u_m(y) = \sum_m T_m \vartheta_m(y), \quad (3.1)$$

$$-\sum_m i\gamma_m T_m \vartheta_m(y) = \sum_m C_m \beta_m \tan(0.5\beta_m h) u_m(y). \quad (3.2)$$

The standing waves inside the slab [the $\cos(\beta_m x)$ in Eq. (1)] are superposition of waves propagating in $+x$ and in $-x$ directions, so one can interpret the in-slab fields as waves circulating within the slab with reflection and transmission at the two slab surfaces; the transverse phase shift for every propagating component is an integer multiple of 2π after a round trip with two reflections. This transversal resonance principle is common for guided modes in arbitrary waveguides.

While the two sets of eigenmodes $\{\vartheta_m\}$ and $\{u_m\}$ each form an infinite-dimensional basis, the high-order ones correspond to fast oscillating fields that are negligible at low frequencies. Therefore, in our numerical calculations, we will perform a truncation down to M terms by expanding the eigenmodes in an M -dimensional basis (details below). In the truncated basis, the transformation between the two bases $\{\vartheta_m\}$ and $\{u_m\}$ is given by to an $M \times M$ matrix \mathbf{P} such that $[u_1(y) \ \dots \ u_M(y)] = [\vartheta_1(y) \ \dots \ \vartheta_M(y)]\mathbf{P}$. In this way, Eq. (3) can be written in matrix form as

$$\mathbf{T} = \mathbf{P}\mathbf{C}, \quad (4.1)$$

$$-i\boldsymbol{\gamma}\mathbf{T} = \mathbf{P}\mathbf{B}\mathbf{C}, \quad (4.2)$$

where $\mathbf{T} = [T_1, \dots, T_{M-1}, T_M]^T$, $\mathbf{C} = [C_1, \dots, C_{M-1}, C_M]^T$, and $\boldsymbol{\gamma}$, \mathbf{B} are diagonal matrices $\boldsymbol{\gamma} = \text{Diag}(\gamma_1, \dots, \gamma_M)$, $\mathbf{B} = \text{Diag}(\beta_1 \tan(0.5\beta_1 h), \dots, \beta_M \tan(0.5\beta_M h))$. Note that the matrix \mathbf{B} is purely real since β_m^2 is real for all m . Eq. (4) is a linear equation group for vectors \mathbf{T} and \mathbf{C} . Substituting Eq. (4.1) into Eq. (4.2) yields $(i\boldsymbol{\gamma}\mathbf{P} + \mathbf{P}\mathbf{B})\mathbf{C} = \mathbf{0}$. Non-trivial solutions exist when

$$f(k_y, \omega) \equiv \|\mathbf{i}\boldsymbol{\gamma}\mathbf{P} + \mathbf{P}\mathbf{B}\| = 0, \quad (5)$$

where $\|\cdot\|$ denotes the determinant of the matrix. Therefore, solving for Eq. (5) for a given k_y yields the dispersion relation $\omega(k_y)$ for the bound states, resonances, as well as BICs. The corresponding field profiles are given by the vectors \mathbf{T} and \mathbf{C} through Eq. (1). At frequencies in the continuum spectrum of the surrounding medium ($\omega > k_y c / \sqrt{\varepsilon_B}$ for a homogeneous medium), some of the γ_m 's are real, and $f(k_y, \omega)$ is generally complex-valued; in such region finding the zeroes of $f(k_y, \omega)$ requires searching for solutions on the lower half of the complex-frequency plane with $\omega_r = \text{Re}(\omega)$ and $\omega_i = -\text{Im}(\omega)$ being the parameters. The imaginary part of the frequency is the decay rate, and the quality factor of the resonance is $Q = \omega_r / (2\omega_i)$.

The transformation matrix \mathbf{P} is deduced from Eq. (2). Inspired by Ref. [24], we expand both sides of Eq. (2) in Fourier series and pick Fourier orders from $-N$ to N (with a total of $M = 2N + 1$ terms). Then, Eq. (2) can be written as matrix equations

$$\mathbf{H}_1 \boldsymbol{\Phi} = \boldsymbol{\Phi} \boldsymbol{\beta}^2, \quad (6.1)$$

$$\mathbf{H}_2 \boldsymbol{\Theta} = \boldsymbol{\Theta} \boldsymbol{\gamma}^2, \quad (6.2)$$

with $\boldsymbol{\beta} = \text{Diag}(\beta_1, \dots, \beta_M)$, and \mathbf{H}_l is an $M \times M$ matrix whose (m, m') -th element is $-(2\pi n/a + k_y)^2 \delta_{mm'} + k_0^2 \xi_l(n - n')$, where $n = m - N - 1$, $n' = m' - N - 1$, and $\xi_l(n)$ is the n -th Fourier coefficient of $\varepsilon_l(y)$. The m -th column of $\boldsymbol{\Phi}$ (or $\boldsymbol{\Theta}$)

contains the $-N$ -to- N Fourier coefficients of u_m (or ϑ_m). Φ and Θ are transform matrices connecting $\{\vartheta_m\}$ and $\{u_m\}$ to the same basis with plane-wave elements, hence $\mathbf{P} = \Theta^{-1}\Phi$. Note that when the permittivity is real and mirror symmetric in y , [$\varepsilon_l(y) = \varepsilon_l^*(y) = \varepsilon_l(-y)$], the matrices \mathbf{H}_l are real symmetric, so β^2 and γ^2 are real; moreover, Φ , Θ , and \mathbf{P} can be chosen to be purely real.

Solving dispersion equation for BIC

BICs arise when the decay rate ω_i of a resonance becomes zero, or equivalently when the amplitudes of the radiating waves vanish: $T_{m'} = 0$ for all the m' with $\gamma_{m'}^2 > 0$. Numerically it can be ambiguous to determine whether ω_i is very small or identically zero. Therefore, we use a slightly modified scheme to look for exact BICs. Define f' as $f' = f|_{(\gamma_{m'}=0)}$: the propagation constants of the radiating waves $\gamma_{m'}$ are artificially set to zero; this function f' is purely real for a lossless dielectric structure that is symmetric in y (where \mathbf{H}_l is real symmetric). A BIC not only satisfies $f = 0$; it also satisfies $f' = 0$ since $T_{m'} = 0$ for a BIC, and from Eq (3.2) it can be seen that setting $\gamma_{m'}$ to zero does not change the solution. Therefore, to search for BICs, we first solve the real-valued equation $f'(k_y, \omega) = 0$ at each k_y for a real-valued frequency ω_i ; the solution also provides a mode profile given by T and C . However, such a mode profile will only satisfy the continuity condition, Eq. (3), if $T_{m'} = 0$. In this work, we study the frequency range where there is only one leaky channel (only one m' with $\gamma_{m'}^2 > 0$), and we perform a root finding with k_y being the free parameter to look for solutions of $f' = 0$ where the amplitude of this radiation channel vanishes, $T_{m'} = 0$. Once found, such a solution will be a true bound state at a purely real frequency and with no radiation.

Results and Discussion

Photonic crystal slab with homogeneous background

In this work we study two systems. The first one is a layered slab in a homogeneous medium (Fig. 1b). It consists of a sequence of dielectric rectangles of size $d \times h$ with permittivity ε_A , surrounded by a homogeneous material with permittivity ε_B . The eigenmodes in the homogeneous medium are simply plane waves with $\gamma_{n+N+1} = \sqrt{\varepsilon_B k_0^2 - (k_y + 2\pi n/a)^2}$ and Θ being an identity matrix. In **Fig. 2a**, the region in dispersion space with one leaky channel (one real $\gamma_{m'}$) is shaded in yellow. In the slab, the

Fourier coefficients of the permittivity is $\xi_1(n) = (d/a)(\varepsilon_A - \varepsilon_B)\text{sinc}(nd/a) + \varepsilon_B\delta_n$. For the basis truncation, we take $M = 21$ Fourier terms and eigenmodes ($N = 10$). As an example, we take $\varepsilon_A = 4.9$, $\varepsilon_B = 1$, $d = 0.5a$, and $h = 1.4a$. The band structure calculated by solving Eq. (5) is shown in Fig. 2a. For even-in- x modes (blue curve), a non-symmetry-protected BIC occurs at $k_y = 0.3156 (2\pi/a)$, $w = 0.4612 (2\pi c/a)$. For odd-in- x modes (green curve), a non-symmetry-protected BIC occurs at $k_y = 0.1640 (2\pi/a)$, $w = 0.6006 (2\pi c/a)$. Symmetry protected BICs can be found at the Γ point ($k_y = 0$), where radiation vanishes because E_z is odd in y for the resonance but even in y for the radiating wave. Fig. 2b shows the quality factor $Q = \omega_r/(2\omega_i)$ of the resonances; as expected, Q diverges at the BICs. Fig. 2c shows the field profiles of the four BICs marked in Fig. 2a,b.

In Fig. 2d, we plot the coefficients \mathbf{C} and \mathbf{T} of the even-in- x non-symmetry-protected BIC. Inside the slab (upper panel), the amplitudes \mathbf{C} are dominated by two propagating modes (shown in red). Outside the slab (lower panel), there is only one propagating mode, and its amplitude vanishes at the BIC. The amplitude of the propagating mode outside the slab is the transmission from the in-slab modes, through Eq. (3). Therefore, the disappearance of radiation arises from destructive interference of the transmission from the in-slab modes, which, as shown in the upper panel, primarily consist of two propagating modes.

Photonic crystal slab with periodically-modulated background

The second system we consider is a PhC slab surrounded by a periodically-modulated background (Fig. 1c). The out-of-slab region has the same period as the slab but with a different fractional volume. We consider $\varepsilon_A = 4.9$, $\varepsilon_B = 1$, $d_1 = 0.5a$, $d_2 = 0.25a$, $h = 1.4a$. Fig. 3a indicates the region with one leaky channel ($\gamma_1^2 > 0$) using yellow shade, and plots the band structure obtained from Eq. (5); the corresponding quality factor is shown in Fig. 3b. In this structure, symmetry-protected BICs can be found both at the Γ point ($k_y = 0$) and at the zone edge ($k_y = \pi/a$) inside the yellow-shaded region; symmetry incompatibility in y prevents the in-slab mode from coupling to radiation, as can be seen from the corresponding mode profile in Fig. 3c.

The preceding examples concern structures where the dielectric is real and symmetric in y , for which the matrices \mathbf{H}_l are real symmetric and so the function f' is real-valued. However, BICs can exist in even more general systems. As long as $\varepsilon_l(-y) = \varepsilon_l^*(y)$, \mathbf{H}_l is real (although not necessarily symmetric and not necessarily Hermitian). In such PT-symmetric systems, if the non-Hermiticity is below the PT-breaking threshold, the eigenvalues and eigenvectors of \mathbf{H}_l can still be real, and the function f' can

still be real-valued. Such systems can also support BICs. However, if the introduction of gain leads to lasing, one will need to account for the nonlinearity resulting from gain saturation³⁶⁻³⁸, which is beyond the linear model considered in this work.

Conclusion

We have presented a mode expansion method that can efficiently and quantitatively describe guided resonances and BICs in PhC slabs, and the method also reveals their underlying formation mechanisms. We find symmetry-protected BICs at the Γ point and at the zone edge, as well as BICs not protected by symmetry. The formalism is easily extendable and applicable to a wide range of structures. This is an attractive approach for the study of guided resonances and BICs in periodic structures.

Acknowledgements

This work was partly supported by the Army Research Office through the Institute for Soldier Nanotechnologies under contract no. W911NF-13-D-0001. B.Z. and M.S were partly supported (analysis and reading of the manuscript) by S3TEC, an Energy Frontier Research Center funded by the US Department of Energy under grant no. de-sc0001299. B.Z. was partially supported by the United States-Israel Binational Science Foundation (BSF) under award no. 2013508. C.W.H. was partly supported by the National Science Foundation through grant no. DMR-1307632. H. C., X. G. and X. L. were partly supported by the National Natural Science Foundation of China under Grants No. 61322501, No. 61574127, and No. 61275183, the Top-Notch Young Talents Program of China, the Program for New Century Excellent Talents (NCET-12-0489) in University, the Fundamental Research Funds for the Central Universities, and the Innovation Joint Research Center for Cyber-Physical-Society System.

[1] Chia Wei Hsu, Bo Zhen, A. Douglas Stone, John D. Joannopoulos, and Marin Soljačić, Bound States in the Continuum. *Nat.*

Rev. Mater (2016).

[2] J. von Neumann, Merkwürdige Diskrete Eigenwerte. *Phys. Z* 30, 465 (1929).

[3] Ulrich R, Modes of propagation on an open periodic waveguide for the far infrared. *Symposium on Optical and Acoustical*

Micro-Electronics, 1: 359-376 (1975).

- [4] Y. Plotnik, O. Peleg, F. Dreisow, M. Heinrich, S. Nolte, A. Szameit, & M. Segev, Experimental observation of optical bound states in the continuum. *Phys. Rev. Lett.*, 107(18), 183901 (2011).
- [5] J. Lee, Bo Zhen, S. L. Chua, W. Qiu, J. D. Joannopoulos, M. Soljačić, & O. Shapira, Observation and differentiation of unique high-Q optical resonances near zero wave vector in macroscopic photonic crystal slabs. *Physical review letters*, 109(6), 067401(2012).
- [6] Chia Wei Hsu, Bo Zhen, J. Lee, S. L. Chua, S. G. Johnson, John D. Joannopoulos, & Marin Soljačić, Observation of trapped light within the radiation continuum. *Nature*, 499(7457), 188-191 (2013).
- [7] Steffen Weimann, Yi Xu, Robert Keil, Andrey E. Miroshnichenko, Andreas Tünnermann, Stefan Nolte, Andrey A. Sukhorukov, Alexander Szameit, and Yuri S. Kivshar, Compact Surface Fano States Embedded in the Continuum of Waveguide Arrays. *Phys. Rev. Lett.* 111: 240403 (2013).
- [8] G. Corrielli, G. Della Valle, A. Crespi, R. Osellame, and S. Longhi. Observation of Surface States with Algebraic Localization. *Phys. Rev. Lett.* 111 (2013).
- [9] Regensburger, Alois, Mohammad-Ali Miri, Christoph Bersch, Jakob Näger, Georgy Onishchukov, Demetrios N. Christodoulides, and Ulf Peschel. Observation of Defect States in PT-Symmetric Optical Lattices. *Phys. Rev. Lett.* 110, no. 22 (2013).
- [10] Originally, BICs are proposed as localized states integrable in all the three dimensions [2]. But in periodic structure, BICs are extended in periodical directions while spatially confined in other directions.
- [11] Shanhui Fan, and J. D. Joannopoulos, Analysis of Guided Resonances in Photonic Crystal Slabs. *Phys. Rev. B* 65 (2002).
- [12] Stephen P. Shipman and Stephanos Venakides, Resonant Transmission near Nonrobust Periodic Slab Modes. *Phys. Rev. E* 71 (2005).
- [13] Suh, Wonjoo, M. F. Yanik, Olav Solgaard, and Shanhui Fan, Displacement-Sensitive Photonic Crystal Structures Based on Guided Resonance in Photonic Crystal Slabs. *Appl. Phys. Lett.* 82, no. 13 (2003).
- [14] D. C. Marinica, A. G. Borisov and S. V. Shabanov. Bound States in the Continuum in Photonics. *Phys. Rev. Lett.* 100 (2008).
- [15] Liu, Victor, Michelle Povinelli, and Shanhui Fan, Resonance-Enhanced Optical Forces between Coupled Photonic Crystal

- Slabs. *Opt. Express* 17 (2009).
- [16] Chia Wei Hsu, Bo Zhen, Song-Liang Chua, Steven G. Johnson, John D. Joannopoulos, and Marin Soljačić, Bloch Surface Eigenstates within the Radiation Continuum. *Light: Science & Applications*, 2(7), e84 (2013).
- [17] Yang, Yi, Chao Peng, Yong Liang, Zhengbin Li, and Susumu Noda, Analytical Perspective for Bound States in the Continuum in Photonic Crystal Slabs. *Phys. Rev. Lett.* 113 (2014).
- [18] Bo Zhen, Chia Wei Hsu, Ling Lu, A. Douglas Stone, and Marin Soljačić, Topological Nature of Optical Bound States in the Continuum. *Phys. Rev. Lett.* 113, no. 25 (2014).
- [19] E.N. Bulgakov, and A.F. Sadreev, Bloch Bound States in the Radiation Continuum in a Periodic Array of Dielectric Rods. *Phys. Rev. A* 90, no. 5 (2014).
- [20] Evgeny N. Bulgakov and Almas F. Sadreev, Light Trapping above the Light Cone in a One-Dimensional Array of Dielectric Spheres. *Phys. Rev. A*, 92(2), 023816 (2015).
- [21] R. Porter and D. V. Evans, Embedded Rayleigh-Bloch Surface Waves along Periodic Rectangular Arrays. *Wave Motion* 43 (2005).
- [22] B. J. Yang, M. S. Bahramy & N. Nagaosa, Topological protection of bound states against the hybridization. *Nature communications*, 4, 1524 (2013).
- [23] J. D. Joannopoulos, S. G. Johnson, J. N. Winn and R. D. Meade, Photonic Crystals: Molding the Flow of Light. 2nd ed. Princeton, NJ: Princeton University Press (2008).
- [24] Weidong Zhou, Deyin Zhao, Yi-Chen Shuai, Hongjun Yang, Santhad Chuwongin, Arvinder Chadha, Jung-Hun Seo, et al, Progress in 2D Photonic Crystal Fano Resonance Photonics. *Prog. Quant. Electron*, 38(1), 1-74 (2014).
- [25] M. Meier, A. Mekis, A. Dodabalapur, A. Timko, R. E. Slusher, J. D. Joannopoulos, & O. Nalamasu, Laser action from two-dimensional distributed feedback in photonic crystals. *Applied Physics Letters*, 74(1), 7-9 (1999).
- [26] M. Imada, S. Noda, A. Chutinan, T. Tokuda, M. Murata, & G. Sasaki, Coherent two-dimensional lasing action in surface-emitting laser with triangular-lattice photonic crystal structure. *Applied physics letters*, 75(3), 316-318 (1999).
- [27] Noda, M. Yokoyama, M. Imada, A. Chutinan & M. Mochizuki, Polarization mode control of two-dimensional photonic crystal

- laser by unit cell structure design. *Science*, 293(5532), 1123-1125 (2001).
- [28] H. Matsubara, S. Yoshimoto, H. Saito, Y. Jianglin, Y. Tanaka & S. Noda, GaN photonic-crystal surface-emitting laser at blue-violet wavelengths. *Science*, 319(5862), 445-447 (2008).
- [29] K. Hirose, Y. Liang, Y. Kurosaka, A. Watanabe, T. Sugiyama, & S. Noda, Watt-class high-power, high-beam-quality photonic-crystal lasers. *Nature Photonics*, 8(5), 406-411 (2014).
- [30] A. A. Yanik, A. E. Cetin, M. Huang et al., Seeing protein monolayers with naked eye through plasmonic Fano resonances. *Proceedings of the National Academy of Sciences*, 108(29), 11784-11789 (2011).
- [31] Bo Zhen, S. L. Chua, J. Lee, et al, Enabling enhanced emission and low-threshold lasing of organic molecules using special Fano resonances of macroscopic photonic crystals[J]. *Proceedings of the National Academy of Sciences*, 110(34), 13711-13716 (2013).
- [32] J. M. Foley, S. M. Young, J. D. Phillips, Symmetry-protected mode coupling near normal incidence for narrow-band transmission filtering in a dielectric grating[J]. *Physical Review B*, 89(16): 165111 (2014).
- [33] H. Friedrich and D. Wintgen, Interfering Resonances and Bound States in the Continuum. *Phys. Rev. A* 32, 3231–42 (1985).
- [34] Shanhui Fan, Pierre R. Villeneuve, J. D. Joannopoulos, M. J. Khan, C. Manolatou and H. A. Haus, Theoretical Analysis of Channel Drop Tunneling Processes. *Phys. Rev. B* 59, no. 24, 15882–92 (1999).
- [35] Chang Sub Kim, Arkady M. Satanin, Yong S. Joe, and Ronald M. Cosby, Resonant Tunneling in a Quantum Waveguide: Effect of a Finite-Size Attractive Impurity. *Phys. Rev. B* 60, no. 15, 10962–70 (1999).
- [36] H. E. Türeci, A. D. Stone, & B. Collier, Self-consistent multimode lasing theory for complex or random lasing media. *Physical Review A*, 74(4) (2006).
- [37] H. E. Türeci, L. Ge, S. Rotter , & A. D. Stone, Strong interactions in multimode random lasers. *Science*, 320(5876), 643-646 (2008).
- [38] L. Ge, Y. D. Chong, & A. D. Stone, Steady-state ab initio laser theory: Generalizations and analytic results. *Physical Review A*, 82(6) (2010)

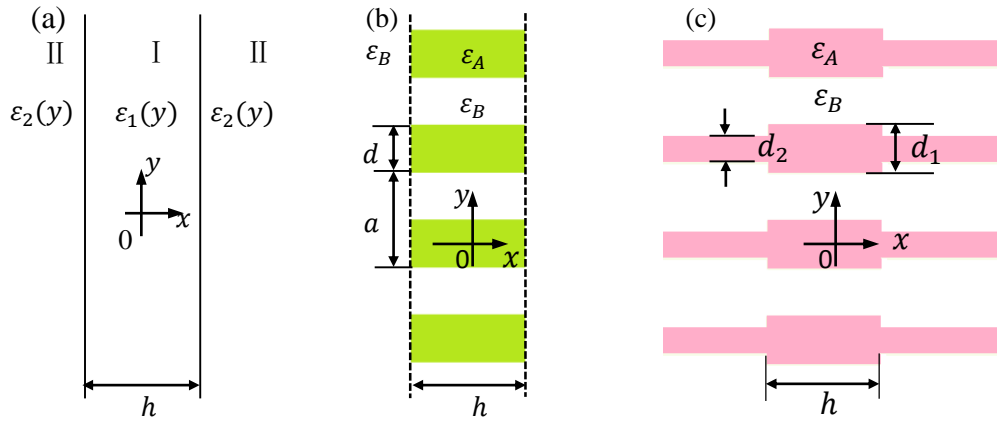


Figure 1 (a) Structure: a 1D photonic crystal (PhC) slab with permittivity $\varepsilon_1(y)$ surrounded by another dielectric media with permittivity $\varepsilon_2(y)$. ε_1 and ε_2 have the same period of a , $\varepsilon_1(y+a) = \varepsilon_1(y)$, $\varepsilon_2(y+a) = \varepsilon_2(y)$. (b) Schematic of a 1D PhC slab embedded in homogeneous dielectric medium. (c) Schematic of a 1D PhC slab embedded in a periodic dielectric background.

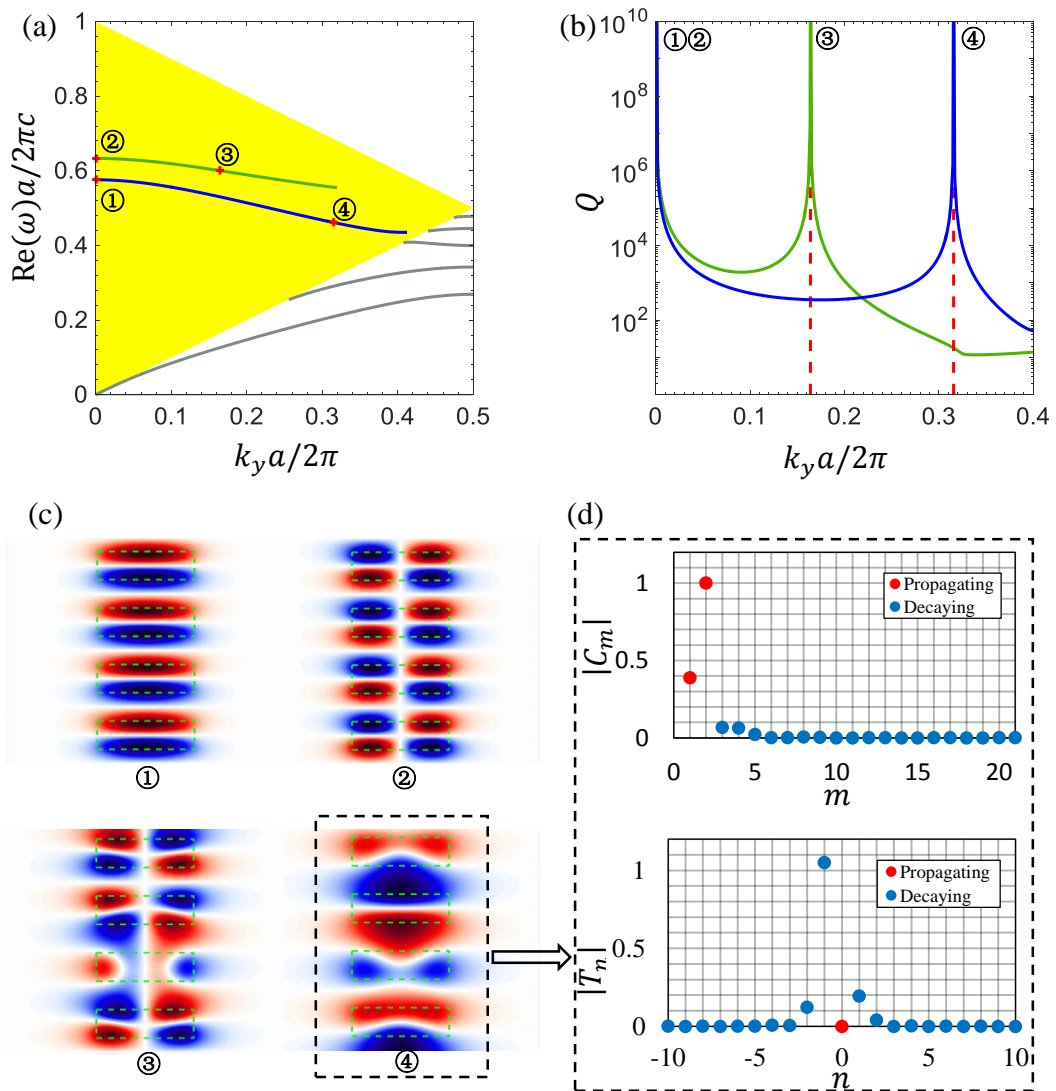


Figure 2 (a) Band structure and (b) quality factors of the guided resonances in the system illustrated in Fig. 1b. (a) Yellow shaded area is where there is only one leaky channel in the surrounding medium. The blue (green) curve is the dispersion of guided

resonances that are even (odd) in x . BICs are marked with red plus signs: ① and ② are protected by symmetry, while ③ and ④ are not. The grey curves are guided modes below the light line. Red dashed lines in (b) mark the location of BICs not protected by symmetry. (c) Electric field patterns of the BICs. (d) Magnitudes of the mode-expansion coefficients in the slab \mathbf{C} (upper panel) and outside the slab \mathbf{T} (lower panel) for the BIC ④. Red circles are components propagating in the x direction (where β_m or γ_m is real); blue circles are evanescent components with imaginary wave vector along the x direction. The structural parameters are: $\varepsilon_2 = 4.9$, $\varepsilon_1 = 1$, $h = 1.4a$, $d = 0.5a$.

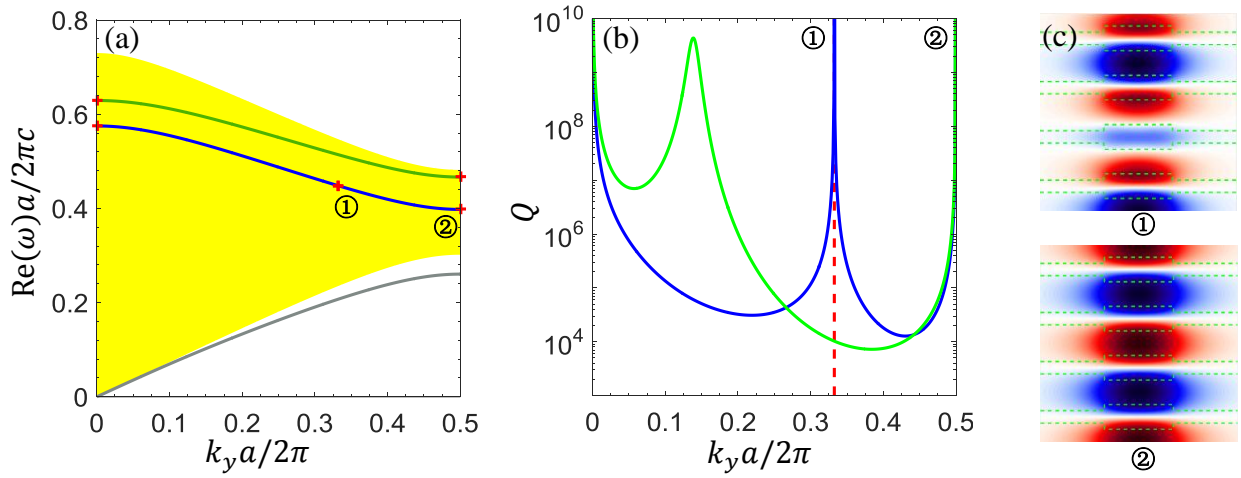


Figure 3 (a) Band structure and (b) quality factors of the guided resonances in the system illustrated in Fig. 1c. The convention is the same as Fig. 2. A symmetry-protected BIC at the zone-edge is labeled by ②, and a BIC not protected by symmetry is labeled by ①. (c) Electric field patterns of the BICs ① and ②. The structural parameters are: $\varepsilon_A = 4.9$, $\varepsilon_B = 1$, $h = 1.4a$, $d_1 = 0.5a$, $d_2 = 0.25a$.